SCIFED Publishers

Research Article **Open Access**

Far-Reaching Field-Mediated Spin and Orbital Interactions

*Heinz Langhals

*Department of Chemistry, LMU University of Munich, Butenandtstr. 13, D-81377 Munich, Germany

Abstract

The extension of interactions of spin and orbital systems were investigated by means of the fluorescence decay of dyes where an interaction was found far beyond the molecular contact or dipole interactions reaching unexpectedly 120 nm or even more. Consequences for spintronics and other spectral regions of electromagnetic radiation such as the NIR and γ-radiation were discussed.

1. Introduction

The interaction of spin and orbital systems is of fundamental importance for many subjects such as quantum chemistry and is becoming even more importance with the development of molecular electronics [1]. The frequency region of visible light at about 0.6 PHz is very attractive for ultra high speed electronics [2]; this touches the upper limit of a safe technology because at even higher frequencies material damage caused by ionisation and thus destruction of chemical bonds becomes more and more dominating [3]. The operating at such high frequencies requires very small electrically conducting structures because of the short wavelengths of electromagnetic radiation emitted at these frequencies. Moreover, high charge carrier mobility is necessary. The combination of these requirements are given by organic chromophores [4] where both resonances in the visible correspond to energetic Eigen values of the absorption and the carrier to effects of polarisability and charge and energy transfer processes. As a consequence, organic molecular chromophores are estimated to be prone for future developments where their wide variability means a special advantage. Generally, the study of the molecular interaction and their coverage concern molecular surroundings form the basis of developments in this field. Two types of interaction of locally energetically excited and thus, information carrying structures should be distinguished: (i) Non resonant interactions where there are no energetic Eigen values of nearer molecular neighbours, and (ii) resonating interactions with surrounding molecules with similar Eigen values where energy may be transported. The interactions will be independently investigated in the liquid phase because of molecular mobility, molecular independence of solutes caused by the solvent shell, and control of the intra molecular distance by the concentration of the solute. Moreover, UV/Vis spectroscopy can be easily and efficiently applied with high precision in homogeneous solution.

2. Materials and Methods

The fluorescent dye S-13 [5, 6] (CAS registry number RN 110590-84-6), the betaine B30 [7] (RN 10081-39-7) and the bichromophore B30dyad [8] (RN 1448254-64-5) were prepared according to the literature.

*Corresponding author: Heinz Langhals, Department of Chemistry, LMU University of Munich, Butenandtstr. 13, D-81377 Munich, Germany. E-mail: Langhals@lrz.uni-muenchen.de; Tel: +49-89-2180-77699

Anhydrous solvents were prepared and purified according to standard procedures [9]. Nile Blue A [10] (RN 3625-57-8) was purchased from Across Organics, product code: 415690100. Chloroform was purchased from Sigma Aldrich (≥ 99.8% with a content of 0.5–1.0% ethanol as stabilizer, product code: 1001744040). S-13 and B30 are also commercially available. UV/Vis spectra were recorded with a Varian Cary 5000 spectrometer, fluorescence spectra with a Varian Cary Eclipse spectrometer; slit width 5 nm unless otherwise specified. Fluorescence lifetimes were measured with a NKT-Laser Super K Extreme EXB-4 from NKT Photonics A/S as light source, an Edinburgh Instruments Ltd. monochromator and detected with a Pico Harp 300 from Pico Quant GmbH in combination with PMA-C 192-N-M photomultiplier. Fluorescence lifetimes were obtained by exponential fitting of the deconvoluted fluorescence decays with a resolution of 8 ps. The fluorescence lifetime equals the negative reciprocal exponent. Excitation and detection wave lengths were steadily the corresponding relative spectral maxima, except the local maximum at 576 nm was applied in case of the detection of S-13. All spectroscopic measurements were carried out in 1.000 cm quartz cuvettes.

3. Non resonant interactions

The betaine dye B30 [7] exhibits a permanent dipole moment in the electronic ground state caused by its special chemical structure; see Figure 1a. Light absorption diminishes the dipole moment in the first electronically excited state [9] where dipolar solvents can solvate and thus stabilise the ground state more efficiently than the excited state.

Figure 1: Molecular Dimensions and Dipole Moments: A) The Betaine Dye B30 (Calculated Dipole 12 Debye), B) The Dyad B30dyad.
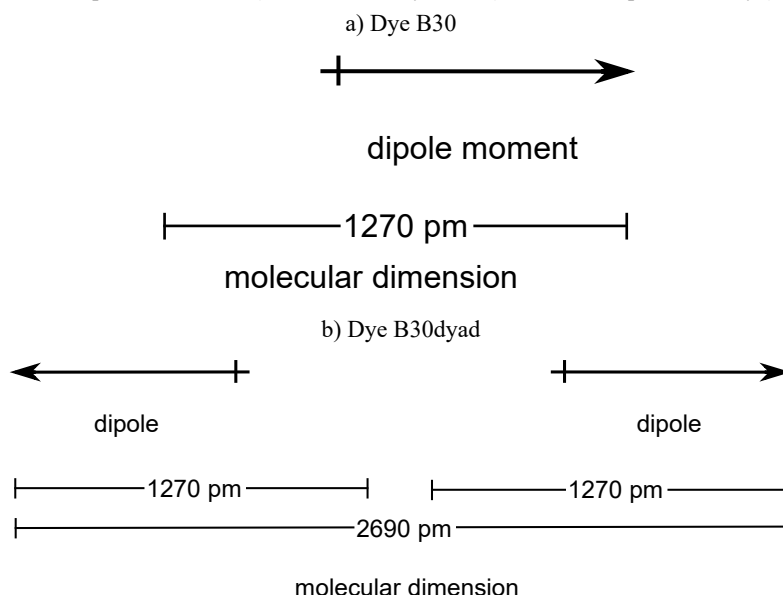
As a consequence, the ground state is more and more lowered in energy with increasing dipolarity of solvents causing a strong negative solvatochromism. Solutions of B30 are in the near infrared absorbing in 1,4-dioxane, green in acetone blue in isoamyl alcohol, violet in ethanol, red in methanol and yellow in water (absorbing near by the UV). The energy of the electronic transition for various solvents can be calculated from λ_{max} of this solvatochromic absorption band by means of equation (1), are known as $E_T(30)$ values, and are applied as a measure for the dipolarity of solvents [11].

$$E_T(30) = 28591[\text{kcal.nm}^{-1}] / \lambda_{max} \qquad (1)$$

The molecular extension of B30 reported in Figure 1a and is only slightly larger than the dimensions of solvent molecules such as toluene with about 590 pm (maximal distance between hydrogen nuclei). The extension of the solvent shell was investigated with dye B30dyad where two chromophores of B30 were chemically linked so that their dipole moments were anti parallel, collinearly arranged such as is shown in Figure 1b. Compensating effects are expected for the interaction with solvent dipoles for large distances; however, independent effects of the individual dipoles in B30dyad were expected for solvent dipoles forming a close solvent shell. The $E_T(30\text{dyad})$ values were determined analogously to the $E_T(30)$ values for various

solvents and a linear correlation between these two solvent-dependent effects were found; see Figure 2. This indicates an identical type of solvent influence on the absorption of both dyes where the slope of this linear correlation indicates the extend of compensation effects. A slope of 0 is expected for complete compensation in B30dyad and a slope of 1 for completely independent operation of the two chromophores in B30dyad. Experimentally, a slope of 1.02 was found, close to unity and thus excluding any compensation effects; see Figure 2.

Figure 2: Linear correlation between $E_T(30)$ (betaine dye B30) and $E_T(30\text{dyad})$ (betaine dye B30dyad) for various pure solvents; slope 1.02, correlation number 0.993 for $n = 20$ solvents. For further information [8].
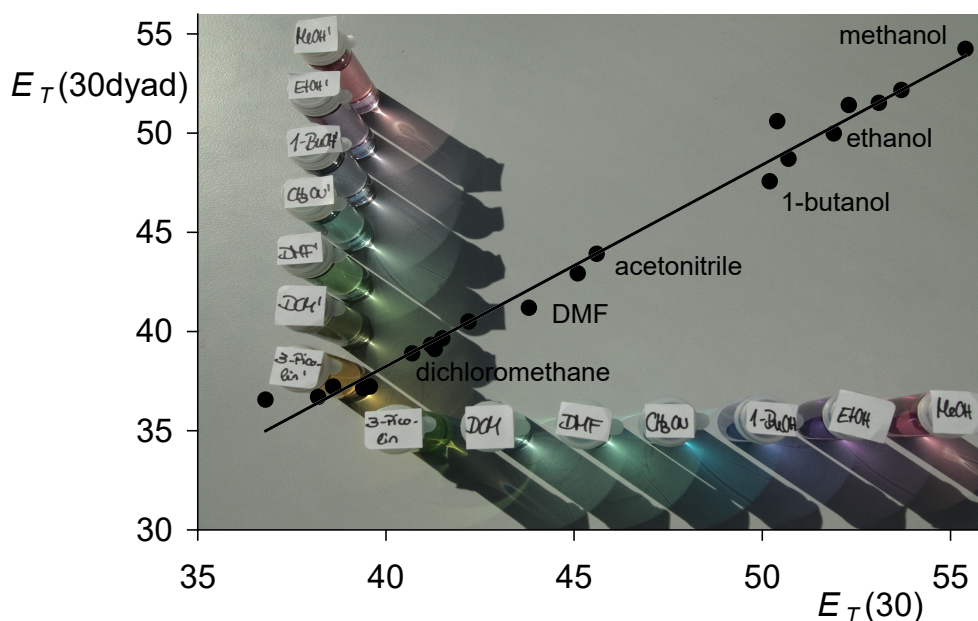
The same result was obtained for other dyads. Thus, the solvent shell must be very thin, not much more than one single molecular layer. As a consequence, non-resonating molecular interactions decline in very short distances and are significant only concerning the nearest molecular neighbours.

4. Resonant molecular interactions

Dipole interactions belong to the most prominent resonant molecular interaction where a theory for the energy transfer was established by Perrin [12] and Förster [13], known as Förster energy transfer (FRET). The investigation of such resonant molecular interactions requires two or more chromophores with similar energetic Eigen values where a resonant energy transfer from the energy donor with shorter wavelengths (chromophore with higher energy of the Eigen value) to the energy acceptor with longer wavelengths (chromophore with lower energy of the Eigen value) proceeds. According to Förster's theory [14] and equation (2), the rate constant k_T of the energy transfer depends on some mathematical and physical constants such as Avogadro's number N_A, the orientation factor κ of the two chromophores, the overlap integral J between the fluorescence spectrum of the energy donor and the absorption spectrum of the acceptor, the fluorescence quantum yield of the donor Φ_D, the fluorescence lifetime of the donor τ_D, and the index of refraction n.

$$k_T = \frac{1000 \cdot (\ln 10) \cdot \kappa^2 \cdot J \cdot \Phi_D}{128 \cdot \pi^5 \cdot N_A \cdot \tau_D \cdot n^4 \cdot R^6} \qquad (2)$$

The distance R between the middle points of donor and acceptor counts in the sixths power in the denominator and causes a fast damping with the separation of donor and acceptor where the Förster-radius with half efficiency can be taken as a measure of damping. This radius hardly exceeds 5 nm for strongly

light-absorbing [15] chromophores. This seems to be the limit in distance concerning intermolecular interactions and thus the target distance for molecular devices.

$$\frac{1}{\tau_0} = A_{u \to l} = 1000 \frac{8\pi \ln(10) c \tilde{v}_{u \to l}^2 n^2}{N_A} \frac{g_l}{g_u} \int \varepsilon \, d\tilde{v} \qquad (3)$$

On the other hand, discrepancies were found with the application of Förster's equation [16] and prompted the investigation of the creation of electromagnetic waves from molecular sources. This was investigated by means of the fluorescence lifetime τ of very strongly fluorescent dyes where τ is close to τ_0, the intrinsic natural lifetime. A theory concerning the fluorescence lifetime was developed by Förster [14] establishing equation (3) and later-on by Sticker and Berg [17] and became popular as the Strickler-Berg-equation. $A_{u \to l}$ means Einstein's transition probability coefficient concerning to the lower

(l) and upper (u) energetic level. N_A means Avogadro's number $\tilde{v}_{l \to u}$ the wave number of the electronic transition, c the velocity of light, n the index of refraction and g_l and g_u the degeneracy's of the lower and the upper energetic state, respectively. The integral concerns the oscillator strengths of the band. Accordingly, τ_0 was attributed to be constant for diluted dye solutions; this was verified with measurements of the fluorescence lifetime of diluted solutions of Nile blue [18] and seems to verify equation (3) even for real systems. However, surprisingly a thorough [19] re-investigation of fluorescence lifetime τ of Nile blue indicated an appreciable dependence of the concentration even in diluted solutions [20].

Nile blue is not the optimal probe for such investigation because of limited stability and fluorescence quantum yield. Thus, the extraordinarily stable perylene derivative S-13 was preferred because of its fluorescence quantum yield very close to unity [21].

Figure 3: a) Left: Dependence of the fluorescence lifetime τ of S-13 in chloroform on the concentration c (circles). Curve: Function $a \cdot \ln(c/c^* + 1) + b$ according to equation (4) with $a = 1.17$ ns, $c^* = 1.17 \cdot 10^{-5}$ mol·L^{-1} and $b = 3.77$ ns. Insert: Linear correlation according to equation (4) (standard deviation 0.015, correlation number 0.9992, coefficient of determination 0.9984, 11 measurements). b) Right: UV/Vis absorption spectra of S-13 in chloroform with propagating dilution. Insert: Precise verification of Lambert-Beer's law by the linear correlation of the absorptivity E as a function of the concentration c; circles: 527 nm, slope $0.810 \cdot 10^5$ L·mol^{-1}, standard deviation 0.49 %, correlation number 0.99995, coefficient of determination 0.9999, 7 measurements) and diamonds: 490 nm (slope $0.504 \cdot 10^5$ L·mol^{-1}, standard deviation 0.44 %, correlation number 0.99988, coefficient of determination 0.9998, 7 measurements).
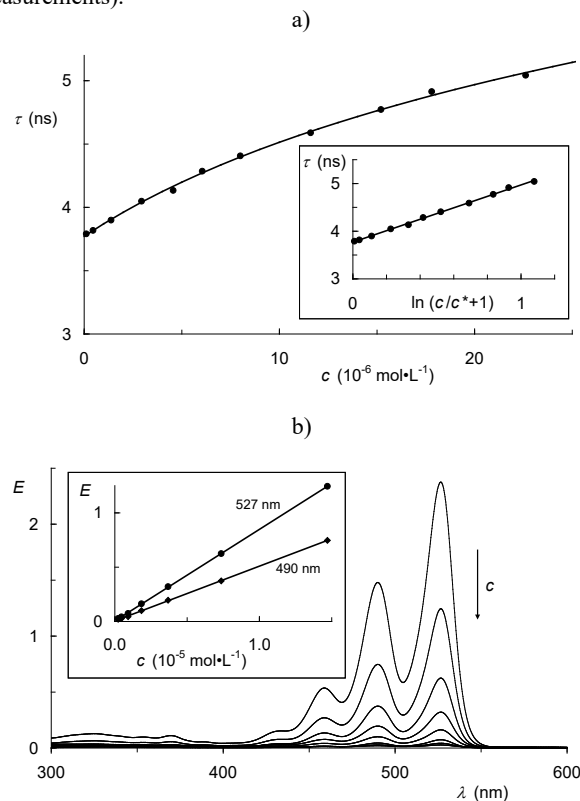
Here Figure 3a indicates an appreciable strong dependence of the fluorescence lifetime τ from the concentration c of S-13; artefacts were excluded by the test of the validity of Lambert Beer's law shown in Figure 3b where the linear concentration dependence of the absorptivity is perfectly fulfilled within the limitation of the spectrometer and so is the concentration dependence of the fluorescence intensity (the shape of both absorption and fluorescence spectra do not alter with the concentration).

$$\tau = a.\ln\left(\frac{c}{c^*}+1\right)+b \qquad (4)$$

The concentration dependence of the fluorescence lifetime τ can be described by equation (4) prior developed for the concentration dependence of solvent effects in binary mixtures [22]; see the curve in Figure 3a and the correlation line in the insert there.

Starting with a concentration of $2 \cdot 10^{-5}$ mol·L^{-1} of S-13 corresponding to an already comparably large mean intermolecular [23] distance of 20 nm one ends up with further dilution to $1 \cdot 10^{-7}$ mol·L^{-1} at a mean distance of more than 100 nm reaching macroscopic dimensions. As a consequence, for practically applied concentrations no isolated molecules are involved in processes with electronic transitions, but ensembles of molecules; this has to be taken into account for many topics such as molecular electronics. On the other hand, the comparably large significant volume of resonant interaction offers many new perspectives such as molecular addressing.

5. Conclusion

Involved volume where electromagnetic waves are generated from molecular excited matter seems to be appreciably larger than commonly thought. Extensions in the order of 1/5 of the vacuum wavelengths and 1/10 taking the refractive index of chloroform into account, respectively, are significant for resonating interactions; the response resembles more a Yagi-Uda antenna [24] than a quantum chemical spin-orbit system. There are consequences for quantum chemical treatments of such interactions because not only macroscopic dimensions were reached, but generally, ensembles instead of isolated molecules are involved. There are not only consequences for processes of interaction of light with matter, but presumably also for other regions of electromagnetic radiation. One may demand if the findings with visible light might be directly applied for such other regions of electromagnetic radiation such as in nuclear chemistry where, for example, the Giant resonance corresponds to a wavelength of about 10^{-13} m. 1/10 of this wavelengths would cover an area of about 10^{-28} m^2 or 1 barn. The region with longer wavelengths of radiation may offer even more new perspectives because the spectral region of molecular vibration covers about 1 until 10 micrometers where 1/10 of these wavelengths is reachable with macroscopic mechanical setups and may link macroscopic and molecular effects.

References

1. Carroll RL, Gorman CB (2002) The genesis of molecular electronics. Angew Chem Int Ed 41: 4378-4400.

2. Langhals H (2014) Handling electromagnetic radiation beyond terahertz using chromophores to transition from visible light to petahertz technology. J Electr and Electron Systems 3: 125.

3. Langhals H (2013) Chromophores for picoscale optical computers. In Sattler, K. (ed.), Fundamentals of picoscience. Taylor and Francis Inc. CRC Press Inc, Bosa Roca/US. 705-727.

4. Zollinger H (2003) Color chemistry: Syntheses, properties, and applications of organic dyes and pigments. John Wiley and Sons, Weinheim.

5. Demmig S, Langhals H (1988) Highly soluble, lightfast perylene fluorescent dyes. Chem Ber 121: 225-230.

6. Homologous of S-13: Highly fluorescent and soluble dyes.[http://www.cup.lmu.de/oc/langhals/Perylenebiscarboximides/index.html]

7. Dimroth K, Reichardt C, Siepmann T, et al. (1963) Über Pyridinium-N-Phenol-Betaine und ihre Verwendung zur Charakterisierung der Polarität von Lösungsmitteln. Justus Liebigs Ann Chem 661: l-37.

8. Langhals H, Braun P, Dietl, C, et al. (2013) How many molecular layers of polar solvent molecules control chemistry? The concept of compensating dipoles. Chem Eur J 19: 13511-13521.

9. Reichardt C, Welton T (2011) Solvents and solvent effects in organic chemistry. 4th ed, Wiley-VCH, Weinheim.

10. Kanitz A, Hartmann H (1999) Preparation and characterization of bridged naphthoxazinium salts. Eur J Org Chem 661: 923-930.

11. Langhals H (2017) Heterocyclic structures applied as efficient molecular probes for the investigation of chemically important interactions in the liquid phase. Chem Heterocycl Compd 53: 2-10.

12. Perrin F (1926) La polarisation de la fluorescence des molécules gazeuses diatomiques. J Phys Radium 7: 390-401.

13. Förster T (1946) Energy transport and fluorescence. Naturwiss 33: 166-175.

14. Förster T (1951) Fluoreszenz organischer Verbindungen. Vandenhoeck and Ruprecht, Göttingen.

15. Kalinin S, Speckbacher M, Langhals H, et al. (2001) A new and versatile fluorescence standard for quantum yield determination. Phys Chem Chem Phys 3: 172-174.

16. Langhals H, Esterbauer AJ, Walter A, et al. (2010) Förster resonant energy transfer in orthogonally arranged chromophores. J Am Chem Soc 132: 16777-16782.

17. Strickler SJ, Berg RAJ (1962) Relationship between absorption intensity and fluorescence lifetime of molecules. Chem Phys 37: 814-822.

18. Jose J, Burgess K (2006) Benzophenoxazine-based fluorescent dyes for labelling biomolecules. Tetrahedron 62: 11021–11037.

19. Langhals H, Schlücker T (2015) The use of dilute chromophore fluorescence decay time for concentration determination. Chem Abstr 163: 714018.

20. Langhals H (2017) A concept for molecular addressing by means of far-reaching electromagnetic interactions in the visible. J Electr and Electron Systems 6: 215.

21. Langhals H, Karolin J, Johansson LBÅ (1998) Spectroscopic properties of new and convenient standards for measuring fluorescence quantum yields. J Chem Soc Faraday Trans 94: 2919-2922.

22. Langhals H (1982) 'Polarity of binary liquid mixtures. Angew Chem 94: 739-749

23. Chandrasekhar S (1943) Stochastics problems in physics and astronomy. Rev Mod Phys 15: 1-89.

24. Yagi H (1928) Beam transmission of ultra short waves. Proc of the IRE 16: 715-740.